Assembly of the ribonucleoprotein complex containing the mRNA of the β-subunit of the mitochondrial H$^+$-ATP synthase requires the participation of two distal *cis*-acting elements and a complex set of cellular *trans*-acting proteins

Javier RICART, José M. IZQUIERDO[1], Carlo M. DI LIEGRO[2] and José M. CUEZVA[3]

Departamento de Biología Molecular, Centro de Biología Molecular 'Severo Ochoa', Universidad Autónoma de Madrid-Consejo Superior de Investigaciones Científicas, Universidad Autónoma de Madrid, 28049 Madrid, Spain

The mRNA encoding the β-subunit of the mitochondrial H$^+$-ATP synthase (β-F1-ATPase) is localized in an approx. 150 nm structure of the hepatocyte of mammals. In the present study, we have investigated the *cis*- and *trans*-acting factors involved in the generation of the ribonucleoprotein complex containing β-F1-ATPase mRNA. Two *cis*-acting elements (β1.2 and 3′β) have been identified. The β1.2 element is placed in the open reading frame, downstream of the region encoding the mitochondrial pre-sequence of the protein. The 3′β element is the 3′ non-translated region of the mRNA. Complex sets of proteins from the soluble and non-soluble fractions of the liver interact with the β1.2 and 3′β elements. A soluble p88, present also in reticulocyte lysate, displays binding specificity for both the *cis*-acting elements. Sedimentation and high-resolution *in situ* hybridization experiments showed that the structure containing the rat liver β-F1-ATPase mRNA is found in fractions of high sucrose concentration, where large polysomes sediment. Treatment of liver extracts with EDTA promoted the mobilization of β-F1-ATPase mRNA to fractions of lower sucrose concentration, suggesting that the structure containing β-F1-ATPase mRNA is a large polysome. Finally, *in vitro* reconstitution experiments with reticulocyte lysate, using either the full-length, mutant or chimaeric versions of β-F1-ATPase mRNA, reveal that the assembly of the β-F1-ATPase mRNA polysome requires the co-operation of both the *cis*-acting mRNA determinants. The present study illustrates the existence of an intramolecular RNA cross-talking required for the association of the mRNA with the translational machinery.

Key words: mRNA localization, oxidative phosphorylation, translation.

INTRODUCTION

The mitochondrial H$^+$-ATP synthase plays a pivotal role in cellular function [1] and in programmed cell death [2–5]. The expression of the nuclear gene encoding the β-catalytic subunit of the F1-ATPase complex is regulated at post-transcriptional levels both during development of the liver [6–9] and in carcinogenesis [10]. The regulation of the expression of the mRNA encoding the β-subunit of the mitochondrial H$^+$-ATP synthase (β-F1-ATPase) involves both the control of the stability [8,10] and of the translational efficiency of the transcript [7–10]. In addition, high-resolution *in situ* hybridization experiments have revealed that the nuclear encoded β-F1-ATPase mRNA appears in electron-dense structures associated with the mitochondrial outer membrane of the hepatocyte [11,12]. The cytoplasmic cluster (approx. 150 nm) of β-F1-ATPase mRNA contains the mitochondrial β-precursor protein associated with the cytoplasmic hsc70 chaperone, as well as proteins from the 60 S ribosomal subunit [13]. Other examples of localized mRNAs appearing in large RNA–protein complexes in the cytoplasm of differentiated mammalian cells have been described [14]. These cytoplasmic granules [14] have been shown to play important roles in the transport, anchoring and translation of the mRNA cargo and to contain most, if not all, of the components of the translational machinery [15,16]. Paradigms of these granules are those containing the β-actin mRNA in neurons and fibroblasts [17], the mRNA of myelin basic protein in oligodendrocytes [15] and 'staufen'-containing granules in neurons [18–20].

At present, little is known about the *cis*- and *trans*-acting components that regulate, post-transcriptionally, the expression of β-F1-ATPase mRNA. However, the control of the translation of the mRNA has been partially characterized and shown to depend on the activity of a non-coding sequence present in the 3′ untranslated region (3′UTR) of the transcript [7,21,22]. We have shown [22] that such a sequence element is required for the efficient translation of the mRNA, and that its function resembles that of the internal ribosome entry sequences (IRES) present in the 3′UTR of the RNAs of certain plant viruses [23–25]. In addition, the control of β-F1-ATPase mRNA translation is regulated by a set of approx. 50 kDa *trans*-acting proteins [3′UTR β-mRNA-binding proteins (3′βFBPs)] that, upon binding to the *cis*-acting 3′UTR element, interfere with its enhancer activity on translation [7]. The binding activity and/or expression of the 3′βFBPs are regulated during development of the liver [7], in carcinogenesis [10] and in a tissue-specific manner [7].

Abbreviations used: ARF1, ADP ribosylation factor 1; β-mRNA, mRNA encoding the β-subunit of the H$^+$-ATP synthase; β1.2BPs, β1.2 β-mRNA-binding proteins; β-F1-ATPase, β-subunit of the mitochondrial H$^+$-ATP synthase; CAT, chloramphenicol acetyltransferase; HDR, high-density region; IDR, intermediate-density region; IRES, internal ribosome entry sequences; Pm, post-mitochondrial; Pn, post-nuclear; Pr, post-ribosomal; 3′βFBPs, 3′UTR β-mRNA-binding proteins; 5′ and 3′UTR, 5′ and 3′ untranslated regions of the mRNA.

[1] Present address: European Molecular Biology Laboratory, Meyerhofstrasse, Heidelberg, Germany.
[2] Present address: Dipartimento di Biologia Cellulare e dello Sviluppo, Università di Palermo, Viale delle Scienze, 90128 Palermo, Italy.
[3] To whom correspondence should be addressed (e-mail jmcuezva@cbm.uam.es).

The localization of RNAs in somatic cells is a mechanism used to define the expression of the mitochondrial H^+-ATP synthase by mediating the targeting of proteins to specific subcellular compartments [26–28]. In this context, findings in lower eukaryotes [12,29–34], as well as in mammalian cells [11,13,35], have shown that both RNA localization and the cytoskeleton are involved in the biogenesis of mitochondria by mediating the targeting of nuclear-encoded proteins into the organelle. The aim of the present investigation was to identify the *cis*- and *trans*-acting elements mediating β-F1-ATPase mRNA cluster formation, i.e. the structure that putatively regulates the metabolic fate of the mRNA [13]. This step is required to establish the link between subcellular localization and translational control of the mRNA, in order to contribute to the elucidation of the post-transcriptional mechanisms that regulate the expression of the mitochondrial H^+-ATP synthase, and hence, influence the biogenesis of mitochondria in mammals. The results obtained illustrate the existence of two distally located RNA-binding domains within the β-F1-ATPase mRNA that co-operate in the assembly of β-F1-ATPase mRNA macromolecular complexes. The β-F1-ATPase mRNA cluster has been partially purified from rat liver extracts and appears to be a large polysome whose assembly requires the participation of the two distal *cis*-acting mRNA elements characterized. Furthermore, the assembly of the β-F1-ATPase mRNA polysome is assisted by a complex set of cellular RNA-binding proteins, some of which display a dual-binding specificity for the two *cis*-acting mRNA domains.

EXPERIMENTAL

Preparation and fractionation of liver homogenates

Adult female (200 g) and timed pregnant albino Wistar rats were fed standard laboratory chow and water *ad libitum*. The foetuses (5.2 ± 0.1 g) were obtained by hysterectomy from cervical dislocated pregnant rats on day 22 of gestation [36]. Adult and foetal livers were collected after decapitation and exsanguination of the animals.

Liver homogenates (1 g) were prepared in 3 ml of a medium containing 0.32 M sucrose, 3 mM magnesium chloride, 2 mM magnesium acetate, 0.1 mM EDTA, 1 mM dithiothreitol and 10 mM Tris/HCl (pH 8.0), and were centrifuged at 2500 ***g*** for 10 min to remove nuclei and unbroken cells [9]. The resulting post-nuclear (Pn) supernatants were either stored frozen at -70 °C until use or subjected to further fractionation. Pn supernatants were centrifuged at 8500 ***g*** for 10 min and the resulting pellet, containing liver mitochondria, and the post-mitochondrial (Pm) supernatant were stored at -70 °C until use. Fresh non-frozen and freeze–thawed Pm supernatants were centrifuged at 180000 ***g*** for 1 h to obtain different versions of the post-ribosomal (Pr) supernatant. To obtain the nuclear fraction, liver homogenates were centrifuged through a 2 M sucrose cushion as described previously [10,37]. The ribosomal fraction of the liver was also obtained. In brief, 1 g of liver was homogenized in 3 vol. of unlabelled polysome buffer (0.25 M sucrose, 0.1 M KCl, 5 mM magnesium acetate, 6 mM 2-mercaptoethanol, 20 mM Tris/HCl, pH 7.6) and the resulting homogenate was centrifuged at 10000 ***g*** for 10 min. Triton X-100 was added to the resulting supernatant to reach a final 1 % (v/v) concentration. The mixture was layered over an equal volume of polysome buffer containing 1.0 M sucrose and centrifuged at 260000 ***g*** for 2 h at 4 °C. The nuclear, mitochondrial and ribosomal fractions were resuspended in a homogenization buffer.

Liver Pn supernatants (2.5 ml) were fractionated on 35 ml sucrose density gradients [24–54 % (w/v)]. The gradients were centrifuged at 145000 ***g*** for 70 min at 4 °C. Fractions (2 ml) were collected from the bottom of the tube at a constant flow rate of 0.5 ml/min. Where indicated, liver Pn supernatants were treated with EDTA (50 μg/ml) for 15 min at 37 °C before loading on to the sucrose gradient. Protein concentration was determined with the Bradford reagent (Bio-Rad protein assay) using BSA as standard.

Plasmids and cloning technologies

The pJMI-β-F1, pJMI3′UTR-β-F1 and pARF1 plasmids, respectively, containing the rat full-length β-F1-ATPase, the 3′UTR of β-F1-ATPase and the bovine ADP ribosylation factor (ARF) cDNAs, have been described previously [7]. The set of plasmids containing different regions of the rat liver β-F1-ATPase cDNA were obtained from the pJMI-β-F1 plasmid after digestion with the appropriate restriction enzymes (Figure 1). The plasmids thus derived were named β1, β1.1, β1.2, β2, β3 and β4 (Figure 1). The pJR3′UTR-α-F1 plasmid, containing the 3′UTR of rat α-F1-ATPase cDNA, and the Dicis-3′βUTR and Dicis-3′αUTR plasmids also contained the chloramphenicol acetyltransferase (CAT) reporter, upstream of the inserts containing the 3′UTRs of the β- and α-F1-ATPase mRNAs, as has been described previously [22]. The β1-CAT-3′βUTR plasmid was obtained from the Dicis-3′βUTR and pJMI-β-F1 plasmids. In brief, the CAT-3′βUTR cDNA, released from the Dicis-3′βUTR plasmid after digestion with *Bam*HI and *Hin*dIII, was subcloned in pcDNA3 vector (Stratagene, Heidelberg, Germany). The resulting plasmid was further digested with *Xho*I and *Eco*RI, and the *Xho*I-end made blunt. The linearized plasmid was ligated with the *Kpn*I–*Eco*RI fragment (β1), released from the pJMI-β-F1 plasmid, after Klenow treatment of the β1 insert to make the *Kpn*-end blunt, generating the β1-CAT-3′β plasmid with the correct orientation downstream of the SP6 promoter. Other plasmids used in the present study were those containing the rat α-F1-ATPase [38] and TRIPLEscript (Ambion, Austin, TX, U.S.A.), the latter containing a 250 bp anti-sense insert of mouse β-actin.

RNA isolation and nucleic acid hybridization

RNA was isolated from 1 ml aliquots of the sucrose-gradient fractions derived from liver Pn supernatants [9]. RNA was either separated by electrophoresis in formaldehyde–(1 %) agarose gels and stained with ethidium bromide or diluted with 300 μl of a solution containing 6.15 M formaldehyde and $10 \times$ SSC [9]. The diluted RNA was denatured by heating at 65 °C for 15 min and applied to GeneScreen membranes, using a slot–blot apparatus. DNA probes were labelled by nick translation. The cDNA probes used were *Eco*RI–*Eco*RI and *Bam*HI–*Bam*HI fragments of the rat liver β- [7] and α-F1-ATPase [38] cDNAs respectively. Hybridization conditions, membrane washing, stripping of labelled DNA probes and the exposure and quantification of hybridization signals were performed as described previously [10]. Standard controls were performed to check that the hybridization signals obtained result from the specific detection of the mRNAs under study. These controls included the pretreatment of the samples with (i) 100 units of DNase I and (ii) 50 mM RNase A (results not shown).

Western blotting of proteins from gradient fractions

Aliquots, containing essentially the same amount of protein (approx. 20 μg) derived from the fractions of the sucrose gradients, were fractioned on SDS/PAGE (12 % gel) after overnight

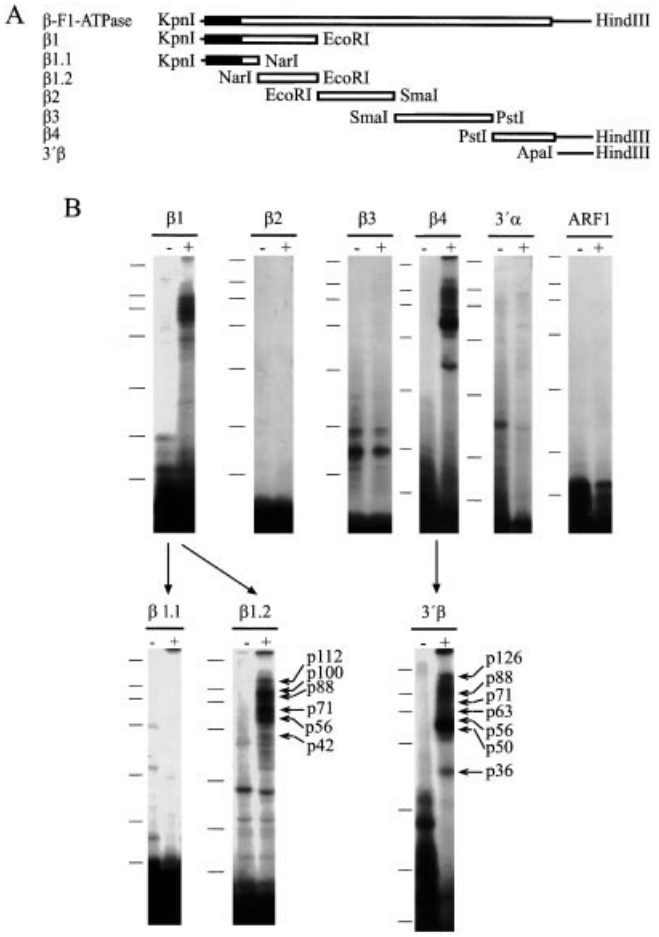

Figure 1 Mapping of the β-F1-ATPase mRNA *cis*-acting elements by UV cross-linking

(**A**) Different fragments of the full-length β-F1-ATPase cDNA from rat liver were subcloned in Bluescript after digestion with the indicated restriction enzymes. The resulting clones (named on the left-hand side) were digested with the restriction enzyme indicated on the right-hand side and used as templates for the *in vitro* synthesis of ^{32}P-labelled riboprobes using T7 viral RNA polymerase. β1 contains the 27 nt of the 5′UTR and the first 514 nt of the coding region. This clone contains the sequence that encodes the presequence of the β-subunit precursor (indicated in black in the schematic diagram). β1.1 contains the 27 nt of the 5′UTR and the first 207 nt of the coding region. This clone also contains the sequence encoding the presequence of the β-subunit precursor (indicated in black in the schematic diagram). β1.2 contains the sequence of β-F1-ATPase cDNA comprised between 208 and 514 nt. β2 contains the sequence of β-F1-ATPase cDNA comprised between nt 515 and 814. β3 contains the sequence of β-F1-ATPase cDNA comprised between nt 815 and 1285. β4 contains the sequence of β-F1-ATPase cDNA comprised between nt 1286 and the end of β-F1-ATPase cDNA. This clone includes the 150 nt of the 3′UTR of β-F1-ATPase mRNA. 3′β contains the 150 nt of the 3′UTR of β-F1-ATPase mRNA. (**B**) UV cross-linking assays were performed using the indicated riboprobes (5×10^5 c.p.m.) in the absence (lane −) and presence (lane +) of 30 μg of protein of post-nuclear extract from foetal rat liver. Other probes used in the present study were those corresponding to the 3′UTR of α-F1-ATPase mRNA (3′-α) and of the coding region of the ARF1. After RNase T1 digestion and UV cross-linking, the samples were fractionated on SDS/PAGE (12.5% gel). The gels were dried and exposed to autoradiographic films. The migration of molecular mass markers (Rainbow mix, RPN 756 from Amersham; 220, 97.4, 66, 46, 30, 21.5 and 14.3 kDa, from top to bottom) is indicated on the left-hand side of each autoradiogram. Arrows and numbers on the right-hand side indicate the migration of the major RNA–protein complexes obtained with the β1.2 and 3′β probes.

dialysis at 4 °C against 10 mM Tris/HCl (pH 7.5). Electrophoretic transfer of the proteins to PVDF membranes and Western blotting were performed as described previously [10]. The primary antibodies used were a rabbit anti-β-F1-ATPase from rat liver [11] and a human antiserum against the P_0, P_1 and P_2 phosphoproteins of the 60 S ribosomal subunit [13]. The secondary antibodies used were goat anti-rabbit IgG (Nordic Immunology, Tilburg, The Netherlands) and goat anti-human IgG (Pierce, Rockford, IL, U.S.A.) peroxidase conjugates.

High-resolution *in situ* hybridization and immunocytochemistry

Fractions derived from the fractionation of Pn supernatants on sucrose gradients were fixed in freshly prepared 4% (w/v) paraformaldehyde in 0.1 M Sörensen phosphate buffer (pH 7.2) for 2 h at 4 °C. After quenching of the free aldehyde groups, the samples were processed for embedding in Lowicryl K4M (Chemise Wercke lowi, Woldkraiburg, Germany) [11]. Gold interference colour ultrathin sections were collected and stored until use. A JEOL 1010 electron microscope was used to observe the sections at 80 kV accelerating voltage.

The *Eco*RI–*Eco*RI fragment of the rat liver β-F1-ATPase cDNA [7] was labelled with digoxigenin by random priming (Boehringer Mannheim, Mannheim, Germany), purified and subsequently used as a probe for *in situ* hybridization experiments, following the method described by Egea and co-workers [11]. For the immunocytochemical detection of digoxigenin, a mouse anti-digoxigenin monoclonal antibody (Boehringer Mannheim) followed by a rabbit anti-(mouse IgG + IgM) (Dako A/S, Golstrup, Denmark) antibody were used. Then, the grids were incubated with Protein A complexed with 10 nm diameter gold particles (BioCell Research Laboratories, Cardiff, U.K.) and finally counterstained with 2% (w/v) uranyl acetate and 1% (w/v) lead citrate.

The immunocytochemical detection of mitochondrial F1-ATPase in gradient fractions was performed following the method described previously for liver samples [13]. A rabbit anti-(F1-ATPase complex) serum was used [36]. Standard controls for the *in situ* hybridization [11] and immunocytochemistry [13] methods were performed.

In vitro synthesis of RNA

The *in vitro* synthesis of RNAs was performed using the MaxiScript kit (Ambion) following the manufacturer's instructions. The synthesis of uncapped riboprobes [7,10] used in UV cross-linking and Northwestern-blot assays was performed using approx. 1 μg of the plasmid as a template that was linearized with the appropriate restriction enzyme. The plasmids used were: β1, digested with *Eco*RI and *Nar*I, to generate the β1 and β1.1 riboprobes respectively; β1.2, digested with *Eco*RI; β2, digested with *Sma*I; β3, digested with *Pst*I; β4, digested with *Hin*dIII; pJMI3′UTR β-F1 and pJR3′UTR α-F1, digested with *Hin*dIII, to generate the β- and α-F1-ATPase 3′UTR riboprobes respectively; pARF, digested with *Apa*I and the linearized commercial TRIPLEscript to generate riboprobes for the sense ARF and anti-sense β-actin respectively.

Capped transcripts using 5′-7mGpppG 5′-cap analogue [7,10] were synthesized for the analysis of the fractionation behaviour of the transcripts on sucrose gradients. The plasmids used in this set of studies had been previously linearized as indicated above. In addition, the following plasmids were used: pJMI-β-F1, digested with *Hin*dIII and *Apa*I, to generate respectively the full-length and 3′UTR-deleted versions of the β-F1-ATPase mRNA; DICIS-3′βUTR, digested with *Apa*I and *Hin*dIII, to generate the CAT and CAT-3′βUTR transcripts respectively; DICIS-3′αUTR and β1-CAT-3′β, digested with *Hin*dIII to generate the CAT-3′αUTR and β1-CAT-3′β transcripts respectively.

Radiolabelled RNA probes were prepared in the presence of 0.1 mM unlabelled UTP plus 50 μCi of [α-^{32}P]UTP (400 Ci/

mmol) (Amersham Pharmacia Biotech). For competition experiments in UV cross-linking and Northwestern-blot assays, unlabelled RNA probes were also synthesized.

UV cross-linking assays

UV cross-linking assays were performed with the modifications described in detail previously [7,10]. Proteins derived from liver fractions, obtained either by differential centrifugation or fractionation on sucrose gradients, and proteins derived from the rabbit reticulocyte lysate were used. When the fractions (1 ml) from sucrose gradients were used, the samples were previously dialysed against 1 litre (5 ×) of 10 mM Tris/HCl (pH 7.5) for 4 h at 4 °C. The cut-off of the dialysis membrane was 6–8 kDa. After dialysis, the samples were freeze-dried and finally resuspended in water and stored at −20 °C until use. Briefly, 35 μg of protein was incubated with radiolabelled probes (1–5 × 10^5 c.p.m.) at 30 °C for 10 min before the addition of 20 units of RNase T1 (Boehringer Mannheim). The reaction mixtures were exposed to 254 nm of UV light (Stratalinker 1800; Stratagene) for 6 min on ice. The RNA–protein complexes were resolved by using SDS/PAGE (10 % or 12 % gels). For competition studies, a 100-fold molar excess of unlabelled RNA was added 10 min before the addition of the radiolabelled RNA [7,10]. After electrophoresis, the gels were dried and exposed to X-ray films.

Fractionation of *in vitro* synthesized RNAs on sucrose gradients

Capped versions of the ^{32}P-labelled RNAs (approx. 2 × 10^6 c.p.m.) were incubated for 20 min at 30 °C with 16 μl of nuclease-treated rabbit reticulocyte lysate (Amersham Pharmacia Biotech) under conditions of mRNA translation [7,22]. After incubation, the reactions were stopped by the addition of cycloheximide (100 μg/ml) and diluted with homogenization buffer supplemented with cycloheximide (100 μg/ml) up to a final volume of 2 ml. The samples were then loaded on to 24–54 % sucrose gradients and processed as described above. The radioactivity recovered in each fraction of the gradient was measured by scintillation counting. Where indicated, incubation reactions were performed in the presence of EDTA (50 μg/ml).

RESULTS

Characterization of *cis*-acting β-F1-ATPase mRNA elements

To characterize the sequence elements on β-F1-ATPase mRNA capable of interacting specifically with proteins from the rat liver, different regions of the β-F1-ATPase cDNA [7] were subcloned for the generation of riboprobes that spanned the entire mRNA sequence (Figure 1A). UV cross-linking assays of the different probes with Pn rat liver extracts revealed that only those derived from the 5′-end (β1 in Figure 1B) and 3′-end (β4 in Figure 1B) of the mRNA produced specific RNA–protein complexes (see also Figures 2 and 3). Probes generated from internal regions of β-F1-ATPase mRNA (β2 and β3 in Figure 1B) or unrelated to this transcript, such as those derived from the 3′UTR of α-F1-ATPase mRNA or from ARF1, did not form specific RNA–protein complexes with liver Pn extracts (Figure 1B).

Sequences on β-F1-ATPase mRNA with the capacity to interact with liver proteins were further mapped after appropriate subcloning and the generation of riboprobes for parts of the β1 and β4 probes (Figure 1A). Interestingly, it was found that those cellular proteins with binding activity for the β1 probe also interacted with its half 3′-end (β1.2 in Figure 1B). In fact, the β1.2 probe provided essentially the same RNA–protein complexes as those obtained with the full-length β1 probe, with major RNA–protein complexes of 112, 100, 88, 71, 56 and 42 kDa (Figure 1B). Likewise, it was found that cellular proteins that interacted with the β4 probe did so by binding the RNA sequence corresponding to the 3′UTR of the RNA (3′β in Figure 1B). In this case, the major RNA–protein complexes observed were of 126, 88, 71, 63, 56, 50 and 36 kDa (Figure 1B). No specific RNA–protein complexes were observed with the *Pst*I–*Apa*I fragment of the β4 probe (Figure 1A; results not shown). Therefore these results indicate the existence of two protein-binding domains on the β-F1-ATPase mRNA. One domain is located towards the 5′-end of the mRNA, placed in the open reading frame and downstream of the region encoding the mitochondrial pre-sequence of the protein, and the other RNA-binding domain is located in the 3′UTR of the transcript.

Cellular proteins binding the 5′-coding region of β-F1-ATPase mRNA

To characterize the subcellular localization of the rat liver *trans*-acting components that interact with β-F1-ATPase mRNA, liver homogenates were fractionated (Figure 2A) and the resulting fractions were further analysed by UV cross-linking with both the β1.2 and 3′β riboprobes. Figure 2 summarizes the results obtained with the β1.2 probe of β-F1-ATPase mRNA. β1.2 β-mRNA binding proteins (β1.2BPs) were present in liver Pn and Pm fractions (Figure 2B). Interestingly, no β1.2BPs were detected when proteins from the mitochondrial and ribosomal fractions were used (Figure 2B). It was observed that the soluble Pr fraction was enriched in proteins forming RNA–protein complexes of 112, 100, 88 and 42 kDa (Figure 2B), whereas RNA–protein complexes of 71, 65, 60 and 56 kDa, present in Pm supernatants, did not appear in the soluble Pr supernatant (Figure 2B). These findings suggest that β1.2BPs belong both to the soluble and non-soluble fractions of the rat liver.

The specificity of the RNA–protein interactions detected was assessed by competition experiments with different riboprobes (Figure 2C). It was observed that addition of an excess amount of the ARF1 riboprobe did not affect the formation of the RNA–protein complexes described above in any of the fractions analysed (Figure 2C). By contrast, the RNA–protein complexes could not be detected at all when there was competition with an excess amount of unlabelled β1.2 riboprobe (Figure 2C). Surprisingly, an excess amount of the unlabelled 3′β probe also competed the formation of the RNA–protein complexes of the soluble fraction (Pr under 3′β in Figure 2C) but not of those of the non-soluble one (Pn and Pm under 3′β in Figure 2C). This latter finding could therefore suggest a dual-binding specificity of the soluble β1.2BPs for the two *cis*-acting elements present in β-F1-ATPase mRNA.

The soluble β1.2BPs were detected and enriched in a fraction containing most of the soluble proteins of rat liver extracts (Figure 2D). Soluble proteins were obtained by sucrose-gradient fractionation of rat liver Pn extracts (see Figure 5C for further details). In contrast, it was not possible to detect non-soluble β1.2 RNA-interacting proteins in gradient fractions (results not shown).

Cellular proteins binding the 3′UTR of β-F1-ATPase mRNA

UV cross-linking experiments with the 3′β probe, using proteins derived from different fractions of the rat liver (see flow diagram in Figure 2A), revealed that the set of 3′βFBPs present in the Pn fraction was enriched in the Pm and Pr supernatants (Figure 3A). No RNA–protein complexes were detected when proteins from the nuclear, mitochondrial and ribosomal fractions were used

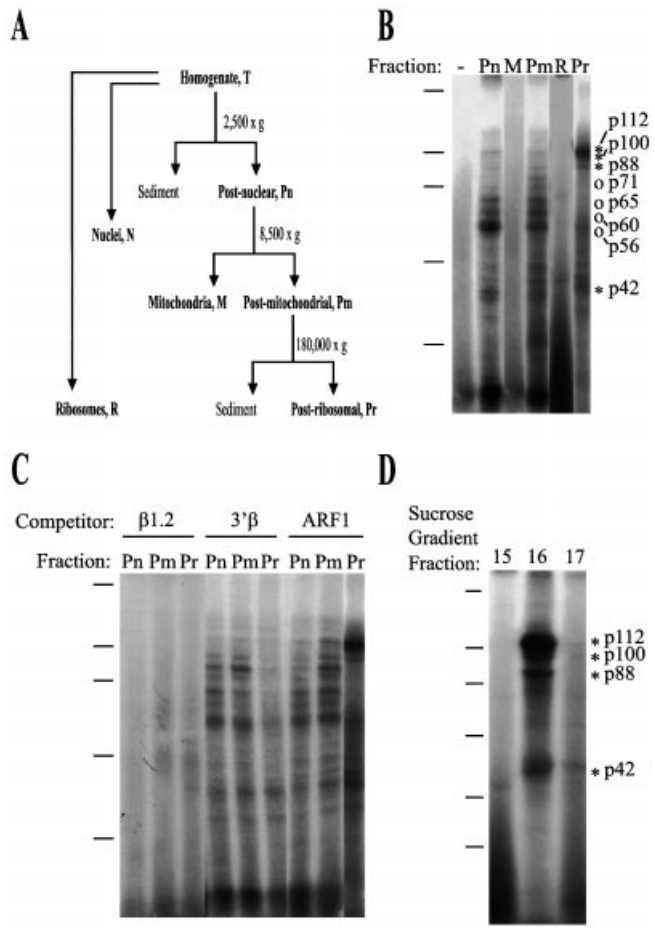

Figure 2 Liver proteins that bind the β1.2 *cis*-acting element

(**A**) Flow diagram illustrating the rat liver subcellular fractions (in boldface) used in the study of β-F1-ATPase mRNA binding proteins. Rat liver homogenates were fractionated by differential centrifugation (**B**, **C**) or by centrifugation on sucrose gradients (**D**). Protein (30 μg) derived from Pn, mitochondria (M), Pm, ribosomal (R) and Pr fractions or from the sucrose-gradient fractions was incubated with 5×10^5 c.p.m. of the ^{32}P-labelled β1.2 riboprobe. Then, the samples were digested with 20 units of RNase T1, UV cross-linked and fractionated on SDS/PAGE (10% gel). The dried gels were exposed to autoradiographic films. The lane labelled '—' indicates the digestion of the probe in the absence of added protein. The migration of the molecular mass markers (220, 97.4, 66, 46, 30 and 21.5 kDa, from top to bottom) is indicated on the left-hand side of each Figure. (**B**) Two major groups of β1.2BPs are present in the liver fractions. Those that become enriched in the non-soluble Pm fraction (identified by ○ on the right-hand side of the Figure) and those enriched in the soluble Pr fraction (identified by asterisks on the right-hand side of the Figure). (**C**) For competition assays, a 100-fold molar excess of the indicated unlabelled riboprobes was added to the UV cross-linking assays. (**D**) UV cross-linking assays reveal the presence of the soluble β1.2BPs in fraction 16 of the sucrose gradients.

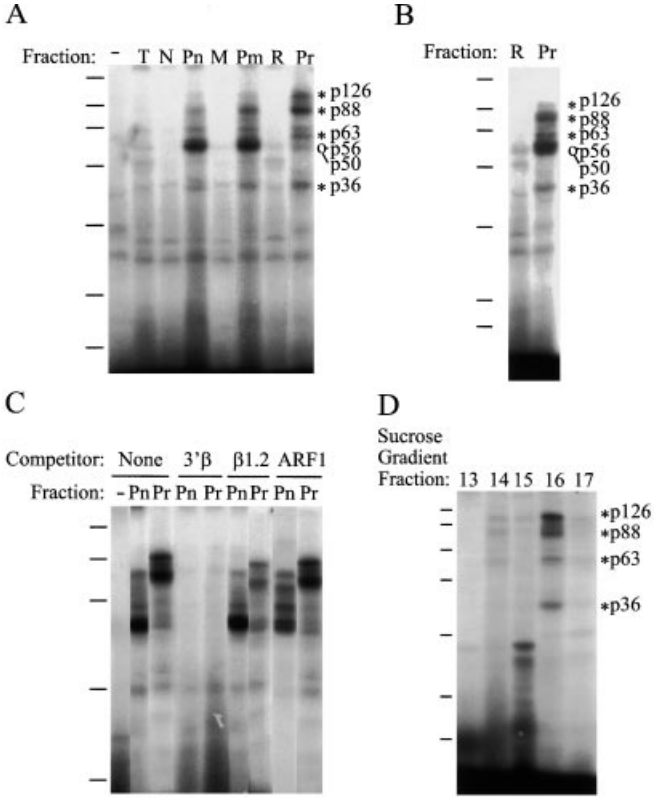

Figure 3 Liver proteins that bind the 3′UTR of β-F1-ATPase mRNA

Rat liver homogenates were fractionated by differential centrifugation (**A**–**C**) or by centrifugation on sucrose gradients (**D**). Protein (30 μg) derived from the liver homogenate (T), nuclear (N), Pn, mitochondrial (M), Pm, ribosomal (R) and Pr fractions or from the sucrose-gradient fractions was incubated with 5×10^5 c.p.m. of the ^{32}P-labelled 3′UTR of β-F1-ATPase mRNA (3′β) riboprobe. Then, the samples were digested with 20 units of RNase T1, UV cross-linked and fractionated on SDS/PAGE (10% or 12.5% gels). The dried gels were exposed to autoradiographic films. The lanes labelled '—', indicate the digestion of the probe in the absence of the added protein. The migration of the molecular mass markers (220, 97.4, 66, 46, 30, 21.5 and 14.3 kDa, from top to bottom) is indicated on the left-hand side of each Figure. (**A**) Two major groups of 3′β binding proteins (3′βFBPs) are present in the liver fractions. Those that become enriched in the non-soluble Pm fraction (identified by a ○ on the right-hand side of the Figure) and those enriched in the soluble Pr fraction (identified by asterisks on the right-hand side of the Figure). (**B**) Fractionation of freeze–thawed Pm liver fractions promotes the appearance of the 50–56 kDa 3′βFBPs in the soluble Pr fraction (identified by a ○ on the right-hand side of the Figure). (**C**) For competition assays, a 100-fold molar excess of the indicated unlabelled riboprobes was added to the UV cross-linking assays. (**D**) UV cross-linking assays reveal the presence of the soluble 3′βFBPs in fraction 16 of the sucrose gradient.

(Figure 3A). It was observed that the soluble fraction was enriched in proteins forming RNA–protein complexes of 126, 88, 63 and 36 kDa. Interestingly, the approx. 50 kDa set of 3′βFBPs mentioned above [7] did not appear in the soluble Pr fraction when fresh non-frozen liver extracts were fractionated (Figure 3A), but did appear in the Pm fraction (Figure 3A). However, when rat liver Pm supernatants were frozen before their fractionation the approx. 50 kDa set of 3′βFBPs appeared as soluble components of the extract (Figure 3B), in agreement with previous findings [7]. Altogether, the findings indicated that 3′βFBPs also belong both to the soluble and non-soluble fractions of the rat liver.

The specificity of the RNA–protein interactions described for the 3′β probe was assessed by competition experiments with different riboprobes (Figure 3C). An excess amount of ARF1 riboprobe was unable to compete the binding of soluble and non-soluble proteins to the 3′UTR of β-F1-ATPase mRNA (Figure 3C). In contrast, an excess amount of unlabelled 3′β probe competed the binding of cellular proteins to the labelled 3′β (Figure 3C). Interestingly, an excess amount of unlabelled β1.2 probe competed the binding of the soluble proteins for the 3′UTR of β-F1-ATPase mRNA (Pr under β1.2 in Figure 3C) but did not significantly affect the binding of proteins from the non-soluble fraction (Pn under β1.2 in Figure 3C). These findings suggest that whereas the major non-soluble 3′βFBPs have binding specificity solely for the 3′UTR of β-F1-ATPase mRNA, the soluble ones have dual-binding specificity,

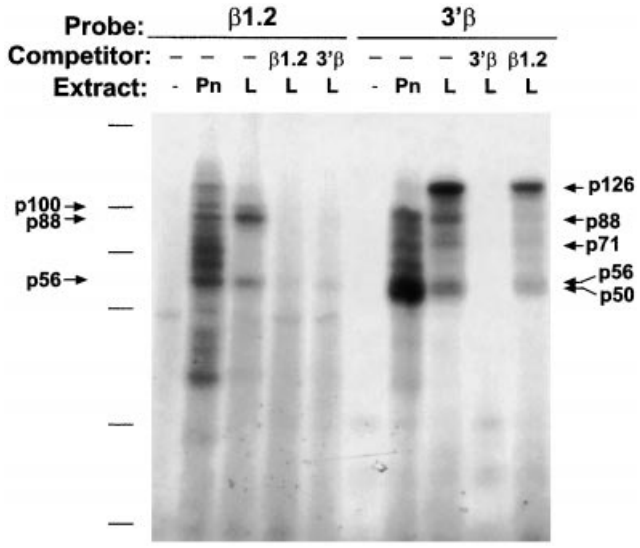

Figure 4 β1.2BPs and 3′βFBPs are also present in rabbit reticulocyte lysate

UV cross-linking assays were performed with 5×10^5 c.p.m. of the ^{32}P-labelled β1.2 and 3′β riboprobes using 30 μg of protein of the Pn foetal liver extract or 2 μl of rabbit reticulocyte lysate (L). For competition experiments, a 100-fold molar excess of the unlabelled β1.2 and 3′β riboprobe was added as indicated. For other details see legends to Figures 2 and 3. The arrows and numbers on the left- and right-hand sides of the Figure indicate the migration of the major RNA–protein complexes formed with the β1.2 and 3′β riboprobes respectively. The migration of the molecular mass markers (220, 97.4, 66, 46, 30 and 21.5 kDa, from top to bottom) is indicated on the left-hand side.

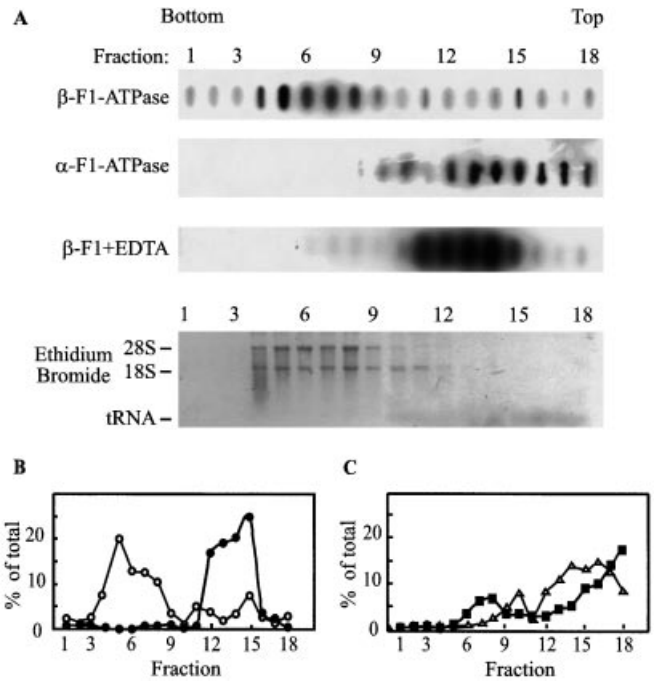

Figure 5 Liver β-F1-ATPase mRNA appears as a large polysome

Pn liver extracts were fractionated on 24–54% sucrose-density gradients. Fractions from the bottom to the top of the sucrose gradient are displayed from left to right. (**A**) After extraction of the nucleic acids, the distribution of the β- and α-F1-ATPase mRNA (on the left-hand side of each blot) was analysed by hybridization procedures. The β-F1 + EDTA blot shows the distribution of β-F1-ATPase mRNA in gradient fractions when the Pn liver extract was previously treated with 50 μg/ml of EDTA, to promote the disassembly of the polysomes. The ethidium bromide-stained gel at the bottom of the panel shows the distribution of the 28 S and 18 S rRNAs in gradient fractions of a non-EDTA-treated extract. (**B**) Effect of the addition of EDTA to the extracts on the distribution of β-F1-ATPase mRNA in sucrose gradients. ○, ● Show the distribution of the mRNA in the absence and presence of EDTA respectively. The autoradiographs for the blots shown in (**A**) were scanned and the percentage of the hybridization signal obtained in each fraction represented. (**C**) Distribution of α-F1-ATPase mRNA (▲) and liver protein (■) in the fractions of the gradient. Note that fraction 5, which is enriched in β-F1-ATPase mRNA (○ in **B**), contains < 1% of the total liver protein loaded in the gradient.

i.e. they are able to interact with both the β1.2 and 3′β determinants of β-F1-ATPase mRNA.

As previously illustrated for the soluble proteins that bind the β1.2 riboprobe (Figure 2D), fraction 16 of sucrose gradients also contained an enriched fraction of the set of soluble 3′βFBPs (Figure 3D). Non-soluble 3′βFBPs, as indicated previously for the set of non-soluble β1.2BPs, were not observed in gradient fractions (results not shown), unless the extract had been previously freeze–thawed (Figure 3B).

Proteins from reticulocyte lysate also form specific RNA–protein complexes with the β1.2 and 3′β RNA *cis*-acting elements

Previously, we have shown that reticulocyte lysate is a helpful system for the identification of mRNA intrinsic features that are essential in controlling β-F1-ATPase mRNA translation [7,22]. Therefore we attempted to characterize the β-F1-ATPase mRNA *trans*-acting elements present in rabbit reticulocyte lysate. UV cross-linking experiments were performed with both the β1.2 and 3′β probes and the profiles of the RNA–protein complexes compared with those obtained when using rat liver Pn extracts (Figure 4). It was observed that the reticulocyte lysate provided fewer RNA–protein complexes with both probes (Figure 4), a finding that might be explained by possible subtle differences in the β-F1-ATPase mRNA sequence between both species and/or by cell-type specific differences in the expression of β-mRNA-binding proteins. However, the RNA–protein complexes of 100, 88 and 56 kDa were obtained with the β1.2 probe and those of 126, 88, 71, 56 and 50 kDa with the 3′β probe. Furthermore, in the case of the 3′β probe it was noted that the binding activity of the 126 kDa complex was increased, whereas that of the 56 and 50 kDa was decreased when compared with rat liver extracts (Figure 4). As illustrated previously for the liver fractions (Figures 2 and 3), the binding of the β1.2 and 3′β elements to proteins of the lysate was competed out with an excess amount of either the β1.2 or the 3′β probes (Figure 4).

Rat liver β-F1-ATPase mRNA forms a large polysome

The rather large number of β-F1-ATPase mRNA interacting proteins present in liver extracts (Figures 1–3), together with previous findings about the high electron density of the structures for the localization of β-F1-ATPase mRNA in the hepatocyte [11,13], suggested that the ribonucleoprotein complex containing β-F1-ATPase mRNA should have a relatively high density compared with other mRNAs, such as the α-F1-ATPase mRNA, whose 3′UTR does not form specific RNA–protein complexes (Figure 1) [22]. To verify this point, rat liver Pn extracts were fractionated on sucrose density gradients and the distribution of the mRNAs encoding the α- and β-subunits of the F1-ATPase complex was analysed. The fractionation of liver Pn supernatants on sucrose density gradients revealed that most of the cellular protein remained in the less-dense region of the gradient (Figure 5C, ■). However, a significant fraction of the protein appeared in fractions 7 and 8 (Figure 5C). Most of β-F1-ATPase mRNA partitioned in the high-density region (HDR) of the

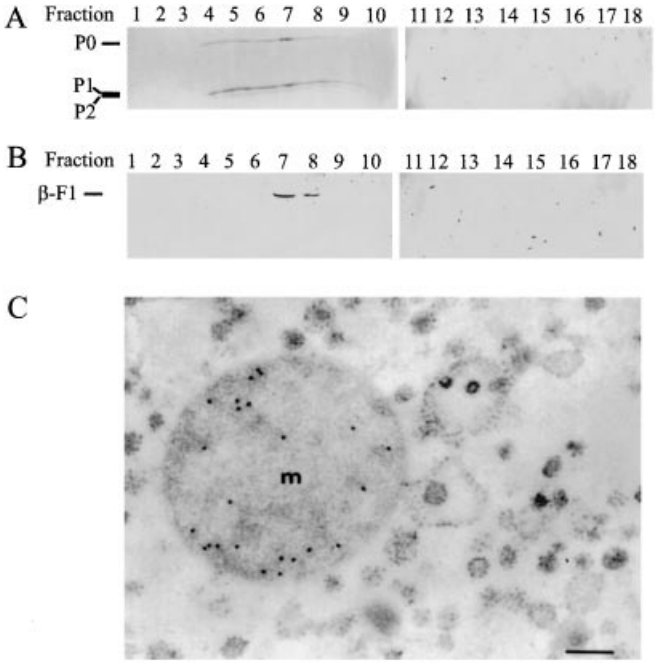

Figure 6 Distribution of ribosomes and mitochondria in sucrose gradients

Aliquots (20 μl) of each fraction of the gradient were fractionated on SDS/PAGE (12.5% gel) and processed for Western blotting. (**A**) Distribution of the P_0, P_1 and P_2 phosphoproteins of the 60 S ribosomal subunit in the fractions. Most of the liver ribosomes distribute to fractions 4–10 of the gradient. (**B**) Distribution of the mitochondrial β-F1-ATPase protein in the fractions. Most of the liver mitochondria distribute to fractions 7 and 8 of the gradient. (**C**) High-resolution immunocytochemistry of fraction 7 of the sucrose gradient. After processing of the sample for electron microscopy, the grids were incubated with a serum that recognizes the mitochondrial F1-ATPase complex. Gold particles exclusively decorated the mitochondria contained in the fraction. m, mitochondria; scale bar, 200 nm.

gradient (Figures 5A and 5B, ○). In contrast, α-F1-ATPase mRNA was located in the less-dense region of the gradient (Figures 5A and 5C, ▲). The distribution of the 28 S and 18 S cellular rRNAs showed that most of the polysomes from rat liver appeared in fractions 4–10 of the gradient (Figure 5A).

The appearance of most of β-F1-ATPase mRNA in the HDR of the gradient, co-fractionating with a large fraction of the cellular 28 S and 18 S rRNAs, suggested that it might form a large polysome. To verify this, rat liver homogenates were pretreated with EDTA before loading on to the sucrose gradient. Treatment with EDTA promotes the disassembly of the polysomes, as assessed by the profound shift in the distribution of the 28 S and 18 S rRNAs into the low-density region of the gradient (results not shown). EDTA treatment results in a complete displacement of β-F1-ATPase mRNA from the HDR of the gradient (Figures 5A and 5B, ●). This finding suggested that the sedimentation behaviour of β-F1-ATPase mRNA from rat liver as a high-density particle is consistent with the formation of a large polysome.

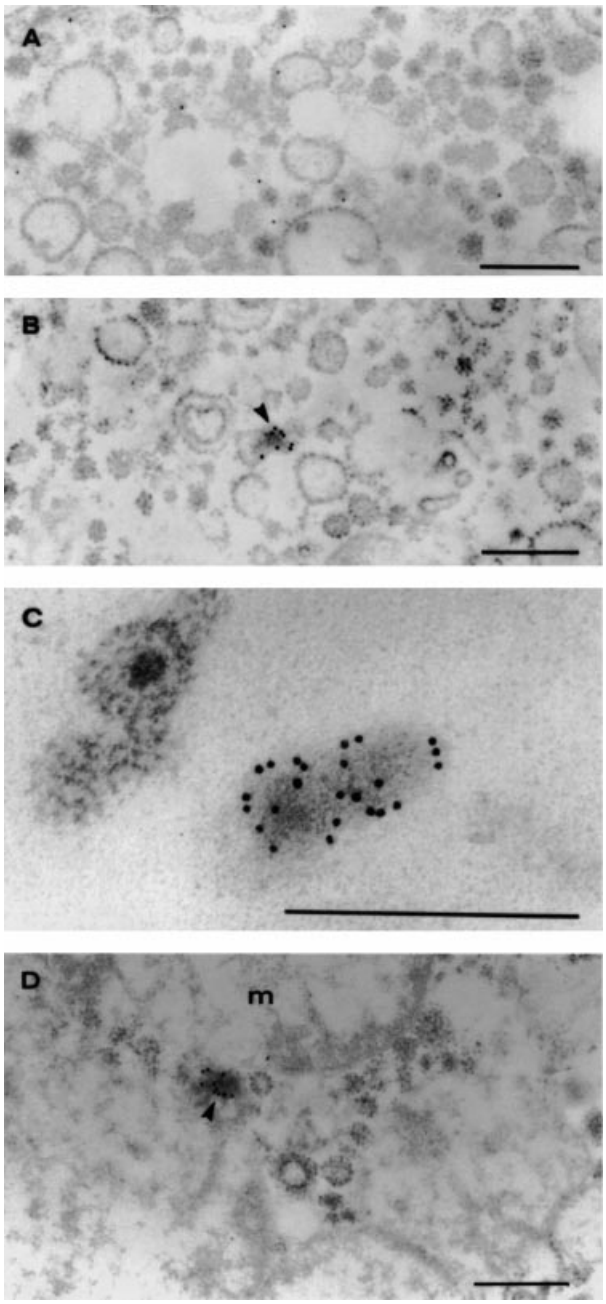

Figure 7 Visualization of β-F1-ATPase mRNA polysomes

High-resolution *in situ* hybridization experiments were performed with fraction 7 of the sucrose gradient using a β-F1-ATPase cDNA probe labelled with digoxigenin as indicated in the Experimental section. (**A**) Control of the hybridization experiment in which the digoxigenin-labelled probe has been omitted. (**B**–**D**) Specific detection of β-F1-ATPase mRNA polysomes using the digoxigenin-labelled probe. The gold particles appeared in clusters that decorated round-shaped electron-dense structures (see arrowheads in **B** and **D**). The β-F1-ATPase mRNA polysomes appeared both 'free' (**B** and **C**) and 'associated' to the mitochondria present in the fraction (arrowhead in **D**). m, mitochondria; scale bars, 500 nm.

Visualization of β-F1-ATPase mRNA polysomes

Western blots of gradient fractions, using antibodies raised against the P_0, P_1 and P_2 phosphoproteins of the 60 S ribosomal subunit [13,39], revealed the co-fractionation of these proteins of the major ribosomal subunit with the cellular 28 S and 18 S rRNA, confirming the distribution of rat liver polysomes in fractions 4–10 of the gradient (Figure 6A). Likewise, Western blots of gradient fractions using antibodies raised against the mitochondrial β-F1-ATPase indicated that the majority of mitochondria partitioned in fractions 7 and 8 of the gradient (Figure 6B). Analysis of fraction 7 of the gradient by immunoelectron microscopy confirmed the presence of mitochondria in this fraction (Figure 6C).

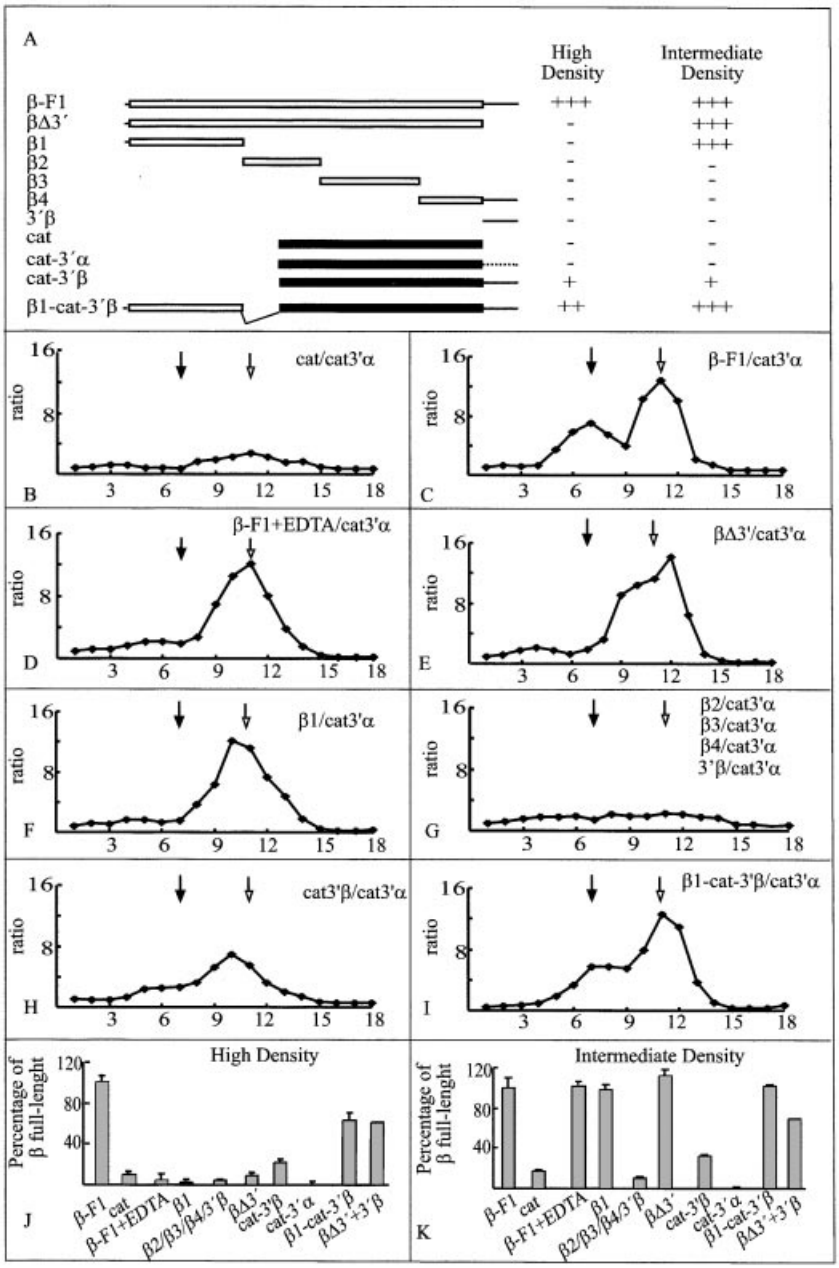

Figure 8 Both the β1.2 *cis*-acting element and the 3′UTR of β-F1-ATPase mRNA are required for the generation of the β-polysome

Different capped and ^{32}P-labelled RNAs (**A**) were synthesized *in vitro* using as templates the plasmids indicated in the Experimental section and viral T7 RNA polymerase. Rabbit reticulocyte lysates were primed with 2×10^6 c.p.m. of each RNA and incubated for 20 min at 30 °C. After incubation, cycloheximide was added to prevent the disassembly of the polysomes. Samples were fractionated on 24–54% sucrose gradients and processed as indicated in the Experimental section. (**A**) Schematic diagrams of the different RNAs used in the fractionation experiments. Their capability to fractionate in the HDR and IDR of the gradient, when compared with the fractionation of the full-length β-F1-ATPase mRNA in these fractions, is indicated as follows: +, approx. 30%; ++, approx. 60% and +++, approx. 100%. (**B**–**I**) Illustrative examples of the ratio of the distribution in the fractions of the gradient of each of the transcripts relative to the distribution of the reference cat-3′α chimaera. The closed and open arrows respectively indicate the HDR and IDR of the gradient, as defined by the peaks of the distribution of the full-length β-F1-ATPase mRNA (see **C**). Note that in (**D**) the lysate was treated with EDTA at a final concentration of 50 μg/ml and in (**G**) the ratio of only one of the RNAs is represented because the other RNAs provided essentially the same flat basal line. For other details see the text. (**J**, **K**) Histograms summarizing the recovery of each RNA studied in the HDR (sum of fractions 5–7) (**J**) and in the IDR (sum of fractions 10–12) (**K**) expressed as percentages of the recovery of the full-length β-F1-ATPase mRNA in those fractions. The results shown are the means ± S.E.M. of 3 or 4 independent experiments. The result of an experiment in which the mutant β-F1-ATPase mRNA that lacked the 3′UTR ($\beta\Delta3'$) was co-fractionated with the 3′UTR of the transcript ($\beta\Delta3'+3'\beta$) is also presented in (**J**) and (**K**).

High-resolution hybridization experiments illustrated the specific detection of β-F1-ATPase mRNA polysomes from rat liver in fraction 7 of the gradient (Figure 7). In fact, clusters of gold particles decorating electron-dense material with a rounded spherical shape were only observed when the labelled β-F1-ATPase probe was used (Figures 7B–7D). Omission of the probe for β-F1-ATPase mRNA provided no significant gold labelling of the structures appearing in the fraction, and the seldom-encountered gold particles always appeared as dispersed signals (Figure 7A). In agreement with previous findings obtained in the

liver *in situ*, the partially purified β-F1-ATPase mRNA polysomes, previously named clusters [11,13], appeared as round-shaped electron-dense structures of approx. 150 nm in diameter (Figure 7C) both 'free' (Figures 7B and 7C) and 'attached' to the mitochondria contained in the fraction (Figure 7D).

The two *cis*-acting elements of the β-F1-ATPase mRNA are required for the generation of the polysome

The specific fractionation behaviour on sucrose gradients of the β-F1-ATPase ribonucleoprotein complex (Figure 5) provided a methodological approach to analyse the role of the *cis*-acting elements in polysome formation. Therefore we studied the fractionation of different RNAs (Figure 8A) on sucrose gradients using reticulocyte lysate as a source of the translational machinery. Preliminary experiments indicated that the maximum fraction of the capped and labelled mRNAs interacting with proteins of the lysate varied from one batch of lysate to another, and was attained 20 min after the addition of the RNAs into the lysate (results not shown). Therefore to illustrate and quantify the specific behaviour of the tested RNAs, (1) the ratio of the percentage of the RNA recovered in each fraction was calculated relative to the percentage of recovery in that fraction of a reference transcript and (2) after incubation for 20 min, cycloheximide was added to the lysate in order to arrest translation elongation and to prevent the disassembly of the polysomes. The samples were subsequently loaded on to sucrose gradients for fractionation. The RNAs used as reference in the present study were the CAT reporter and the chimaera CAT-3′α, which contained the 3′UTR of α-F1-ATPase mRNA downstream of the CAT reporter. It should be mentioned that none of the transcripts used as reference in the present study has a sedimentation behaviour similar to that of the β-F1-ATPase mRNA (Figure 5; results not shown).

The distribution on gradient fractions of the two reference mRNAs, CAT and CAT-3′α, was essentially the same throughout the gradient, as shown by the absence of peaks in the CAT/CAT-3′α ratio (Figure 8B). In contrast, the β-F1-ATPase/CAT-3′α (Figure 8C) or β-F1-ATPase/CAT (results not shown) ratios revealed that β-F1-ATPase mRNA was distributed in two peaks: the HDR, corresponding to the peak at fraction 7, and the intermediate-density region (IDR), corresponding to the peak at fraction 11 of the gradient (marked by a closed and open arrow in Figures 8B–8I respectively; see also Figures 8J and 8K for quantifications). Treatment of the lysate with EDTA, previous to its loading in the gradient, promoted the disappearance of β-F1-ATPase mRNA from the HDR but not from the IDR (Figures 8D, 8J and 8K). This finding suggests that the HDR of the gradient corresponds to the polysome fraction of the lysate. In addition, the results obtained with the full-length β-F1-ATPase mRNA, both in the presence and absence of EDTA (Figures 8C and 8D), suggest that the partitioning of the transcript in the IDR must result from the specific interaction of the transcript with components of the lysate that the reference RNAs do not establish (Figure 8B).

The fractionation of a mutant β-F1-ATPase mRNA (βΔ3′) lacking the 3′UTR of the wild-type transcript, revealed that the 3′UTR deletion was sufficient to prevent the fractionation of the transcript into the HDR (Figures 8E, 8J and 8K). However, the βΔ3′ construct retained the ability to fractionate in the IDR of the gradient (Figures 8E, 8J and 8K). Interestingly, fractionation of the βΔ3′ mutant, when the 3′UTR of β-mRNA was added in *trans*, partially restored the capability of the βΔ3′ mutant to fractionate in the HDR of the gradient (see βΔ3′ + 3′β histogram in Figures 8J and 8K).

To define the sequence determinants on β-F1-ATPase mRNA responsible for its biphasic behaviour on centrifugation (Figure 8C), the distribution pattern of capped riboprobes spanning different β-F1-ATPase mRNA regions was analysed. It was observed that only the β1 mRNA was mobilized to the IDR of the gradient (Figure 8F). Other sequence regions of the β-F1-ATPase mRNA, such as β2, β3, β4 and the 3′-UTR alone (3′β), lacked any differential activity when compared with the reference mRNAs (Figures 8G, 8J and 8K). These findings indicate that localization of the mRNA in the IDR of the gradient depends on determinants residing on the β1 region of the transcript. It should be noted that none of the β-F1-ATPase mRNA fragments mobilized by itself into the HDR (Figures 8F, 8G, 8J and 8K). This supports the view that other *cis*-acting determinants, probably placed at the 3′UTR (Figure 8E), are involved in the recruitment of the mRNA to the HDR. In this context, it was surprising that neither the β4 nor 3′β RNAs was mobilized into the HDR and IDR fractions of the gradient, even though the 3′UTR is required to generate the HDR fraction (Figure 8E). This finding suggests that the 3′UTR is a necessary but not a sufficient element to promote the sedimentation of the mRNA in the HDR, thus suggesting that elements placed upstream of the 3′UTR of β-F1-ATPase mRNA are required to define this property. Hence, we developed a construct in which the 3′UTR of β-F1-ATPase mRNA was placed downstream of the CAT reporter (CAT-3′β). At variance with the capped β4 RNA, the CAT-3′β RNA provides a 5′UTR and an initiation codon within the proper context for mRNA translation. Interestingly, the chimaeric CAT-3′β mRNA was mobilized into the HDR and IDR fractions, albeit with much less efficiency than β-F1-ATPase mRNA (Figure 8H).

Finally, we analysed the behaviour of a chimaeric CAT mRNA that contained the β1 sequence in its 5′-end and the 3′UTR of the β-F1-ATPase mRNA in its 3′-end (Figure 8I). The chimaeric β1-CAT-3′β mRNA efficiently partitioned both in the IDR and HDR of the gradient, resembling the distribution pattern of the wild-type β-F1-ATPase mRNA (compare Figure 8I with Figure 8C; see also Figures 8J and 8K). Altogether, these results indicate that the β1 element recruits the mRNA to the IDR and, in the presence of the 3′UTR, a fraction of the mRNA present in the lysate is mobilized into the HDR. Therefore the results illustrate a co-operation and/or cross-talk between the *cis*-acting elements of the transcript to define the association of β-F1-ATPase mRNA with large polysomes.

DISCUSSION

In the present study, we have identified and partially purified, on sucrose gradients, the subcellular structure containing the mRNA of the β-F1-ATPase from rat liver. We suggest that such a structure is a large polysome. We show that the assembly of the β-polysome requires the co-operation of two distal *cis*-acting elements, one located at the beginning of the open reading frame of the mature protein and the other at the 3′UTR of the mRNA. This finding illustrates the requirement of a specific intramolecular RNA cross-talk for mediating the association of the mRNA with the translational machinery. In addition, we have characterized the different *trans*-acting components of the rat liver and rabbit reticulocyte lysate that specifically interact with both the *cis*-acting determinants. Interestingly, it is shown that a soluble protein, approx. 88 kDa, present in both types of cellular extracts, has binding specificity for the two *cis*-acting elements involved in the polysomal localization of the mRNA.

The β-F1-ATPase mRNA cluster is a large polysome

A dissimilar subcellular distribution of the nuclear transcripts encoding mitochondrial proteins has been observed in *Saccharomyces cerevisiae* [29,31,33,40]. In mammals, *in situ* hybridization experiments also indicated that nuclear transcripts encoding subunits of oxidative phosphorylation have different subcellular localizations [11]. The differences in the sedimentation behaviour on sucrose gradients of the α- and β-F1-ATPase mRNAs observed in the present study (Figure 5) confirmed the above findings and posed the intriguing question as to why transcripts that are involved in the expression of the same molecular complex are so differently located. Mitochondrial precursor proteins have been classified into two groups depending upon their cytosolic energy requirements for import into mitochondria [41] and upon association of the mRNAs with free and mitochondrial-bound polysomes [40]. It is tempting to suggest that the differences in the subcellular localization [11] and fractionation behaviours (Figure 5) of the α- and β-F1-ATPase mRNAs might reflect differences in the mechanism of translation and mitochondrial import of the precursor proteins encoded by the two transcripts.

The co-fractionation of β-F1-ATPase mRNA with components of the 60 S ribosomal subunit and, most importantly, the release of β-F1-ATPase mRNA to less-dense regions of the gradient upon disassembly of the polyribosomes, strongly suggest that β-F1-ATPase mRNA clusters represent a subfraction of the large rat liver polysomes. This finding is also supported by the fact that β-F1-ATPase mRNA co-localizes with 60 S ribosomal proteins in the liver *in situ* [13]. Altogether, the findings strongly support that the cluster structure of the β-F1-ATPase mRNA is the site for its translation.

The *cis*-acting elements on β-F1-ATPase mRNA

Two *cis*-acting elements on β-F1-ATPase mRNA have been characterized with the ability to establish specific interactions with cellular proteins from rat liver extracts and rabbit reticulocyte lysate. There are other examples in the literature where *cis*-acting elements involved in mRNA localization and/or metabolism are also placed, in addition to the 3′UTR, in both the 5′UTR and in the open reading frame of the transcripts [42–46]. In this context, recent findings [31] have indicated the existence of apparent redundancy in the *cis*-acting information required for the generation of mitochondrial-bound polysomes in yeast. In that study [31], it was shown that both the pre-sequence and the 3′UTR of the ATM1 mRNA have the information required for the specific localization of the mRNA. At variance with this observation, the polysomal localization of β-F1-ATPase mRNA in mammalian cells requires a functional co-operation of the two *cis*-acting elements characterized.

It has been reported that the translation of a 3′UTR β-F1-ATPase mRNA deletion mutant was negligible when compared with the translation of the full-length transcript [7,22]. In addition, the 3′UTR of β-F1-ATPase mRNA has been shown to function as an enhancer of mRNA translation, both of the β-F1-ATPase mRNA itself [7,22] and of different chimaeric reporter RNAs [21,22]. In fact, the 3′UTR of β-F1-ATPase mRNA, when placed in the intercistronic region of dicistronic constructs, has a strong activity as an internal ribosome entry sequence [22], i.e. it is able to promote the recruitment of translation machinery. The capacity of the 3′UTR to recruit the mRNAs into polyribosomes (Figures 8H and 8I) helps to explain the role of this *cis*-acting element as an enhancer of mRNA translation. In fact, the 3′UTR of β-F1-ATPase mRNA is a required *cis*-acting element for the generation of a large polysome (Figure 8). Interestingly, this observation is in agreement with a report in which cellular RNAs that contain IRES located at the 5′UTR were also found localized in large polysomes [47]. These findings therefore suggest that the increased translation of cellular mRNAs containing 3′ [7,22] or 5′ located [47] IRES do so by promoting the recruitment of the mRNA into polyribosomes.

To recruit the mRNA into polysomes the 3′UTR requires a 5′-end on the mRNA with the proper context for mRNA translation (compare Figure 8G with Figure 8H; for quantification see Figure 8J). These findings suggest that the 3′UTR of β-F1-ATPase mRNA establishes some kind of molecular cross-talk with elements that interact with the 5′-end of the transcript. However, it appears that the efficiency of this interaction, measured by the percentage of recovery of the mRNA in polysomes, is very much enhanced if the upstream *cis*-acting element of β-F1-ATPase mRNA is provided (compare Figure 8H with Figure 8I; for quantification see Figure 8J), suggesting that such cross-talking is efficiently mediated by any of the *trans*-acting components with which the β1.2 *cis*-acting element interacts (Figures 2 and 4). It is at present clear that translationally competent mRNAs are closed circular molecules in which the 5′- and 3′-ends of the RNA are in close spatial proximity. In most eukaryotic mRNAs, the transcript is circularized by the communication established between the 5′-cap and the polyadenylated [poly(A)$^+$] tail of the mRNA via the interaction of these *cis*-acting elements with their respective *trans*-acting components [48–50]. In the case of certain non-poly(A)$^+$ viral mRNAs the communication between the 5′- and 3′-ends of the mRNA, and hence circularization of the transcript, is mediated by a specific *trans*-acting protein that recognizes *cis*-acting elements located at both the 5′- and 3′-UTRs of the mRNA [51]. Recently [45], an additional mechanism (kissing mechanism) has been reported to provide translational competence to uncapped non-poly(A)$^+$ viral mRNAs that involves the base-pairing between 5′- and 3′-UTRs of the mRNA. The interaction between the β1.2 and 3′UTR *cis*-acting elements described for the mammalian β-F1-ATPase mRNA provides an additional indication that efficient mRNA translation requires the intramolecular communication of different *cis*-acting elements present in the mRNA.

The *trans*-acting factors of β-F1-ATPase mRNA

The large number of interactions established between β-F1-ATPase mRNA and liver proteins provides an indication of the complexity of the post-transcriptional mechanisms (localization/stability/translation) that regulate the cytoplasmic expression of the mammalian β-F1-ATPase mRNA. Most of the liver β-F1-ATPase mRNA fractionates as a large polysome (Figure 5A), whereas in reticulocyte lysate only a fraction of the β-F1-ATPase mRNA is recruited into the large polysomal region of the gradient (compare the size of the two peaks in Figure 8C). This finding could indicate that a factor involved in the assembly of the β-polysome is present in limited amount or activity in the reticulocyte lysate. In any case, the presence of a set of RNA-interacting proteins with similar molecular mass in both systems suggests that the β-F1-ATPase mRNA *cis*- and *trans*-acting components might also exist and participate in the control of the expression of the transcript in other cell types and in other mammals.

The finding that a mutant β-F1-ATPase mRNA that lacks the 3′UTR is efficiently mobilized into large polysomes when the 3′UTR of β-F1-ATPase mRNA is added in *trans* to the lysate system (Figure 8J), i.e. not covalently linked to the messenger, strongly suggests that partitioning of the mRNA into the HDR

is promoted by the recognition of the β1.2 and 3′β elements by a common protein or protein complex that provides the RNA-recognition domains for both elements. The recruitment of the RNA–protein complex formed into the HDR of the gradient thus requires the incorporation of additional proteins into the primary RNA–protein complex, that defines the IDR. Presumably, such incorporation could be triggered by conformational changes on the primary RNA–protein complex [52] as a result of acquiring, after binding of the 3′UTR, a competent conformation for the generation of the polysome. It is tempting to speculate that the approx. 88 kDa RNA–protein complex, present in liver and reticulocyte lysate, having the capacity to interact with both the β1.2 and 3′β elements (Figures 2–4), is a candidate to play a major role in determining the localization of the β-F1-ATPase mRNA in polysomes. This observation is in line with the localization-dependent translation of *oskar* mRNA. This also requires a protein that has a dual-binding specificity for two distal *cis*-acting elements of the transcript [44]. As suggested recently for the localization/translation/degradation of other mRNAs [53], the protein–RNA bridging of distal regions of the β-F1-ATPase mRNA might imply that β-polysomes are dynamic structures in which the binding of regulatory proteins, to either *cis*- or *trans*-acting determinants, could specify the fate and/or functionality of the mRNA within the cell.

In this context, our results strongly support that the set of approx. 50 kDa 3′βFBPs, present in the non-soluble fraction of the liver (Figure 3A), are involved in the repression of β-F1-ATPase mRNA translation [7,10]. The presence of this set of proteins in the Pm fraction of the liver as non-soluble components (Figure 3A), unless the samples have been previously freeze–thawed (Figure 3B; see [7]), suggests that such inhibitors do form a portion of the β-polysome bound to their target *cis*-acting element [7].

β-polysomes and mitochondrial protein import

Several pieces of evidence suggest that mitochondrial protein import could occur *in vivo* by a co-translational import mechanism. The preferential accumulation and distribution of certain nuclear-encoded mRNAs on mitochondrial bound polysomes [11,13,29,31,33,40], the tight coupling between protein translation and membrane translocation [54–56] and the involvement of RNA-interacting proteins that play a role in nucleocytoplasmic traffic of RNAs [12,30,32,34], all favour this argument. The physical association between β-F1-ATPase mRNA polysomes and mitochondria (present study and [11,13]) also suggests a functional link between the sorting and translation of the mRNA and the import of the encoded protein. Since the β1.2 *cis*-acting element is placed immediately downstream of the sequence encoding the mitochondrial targeting signal of the β-precursor (Figure 1), it is tempting to speculate that its functional role within the cellular context could be to arrest the synthesis of the mitochondrial protein until the β-F1-ATPase mRNA polysome reaches the mitochondrial membrane, resembling in some way the mechanism and sorting pathway of mRNAs translated and anchored at the membranes of the endoplasmic reticulum [57,58]. This mechanism would imply a localized translation of the β-F1-ATPase mRNA in order to achieve a high-fidelity protein targeting. The purification and cloning of β-F1-ATPase mRNA *trans*-acting factors is nowadays the major goal of our laboratory in order to provide mechanistic insights to the post-transcriptional regulation of the biogenesis of mammalian mitochondria.

We are grateful to Dr J. Satrústegui and Dr J. Zapata for a critical review of the manuscript. We are indebted to C. San Martín for her contribution in the electron microscopy work. We thank M. Chamorro for technical assistance. J.R. was a predoctoral fellow from the Plan de Formación de Personal Investigador, and C.M.D.L. was the recipient of a Fellowship for Foreign Scientist, both sponsored by the Spanish Ministerio de Educación y Cultura. This work was supported by grants PB97-0018 and 08.1/0006/1998, from Dirección General de Enseñanza Superior e Investigación Científica, Spain and Dirección General de Investigación (Comunidad de Madrid), Spain respectively. Centro de Biología Molecular 'Severo Ochoa' receives an institutional grant from Fundación Ramón Areces, Spain.

REFERENCES

1 Boyer, P. D. (1997) The ATP synthase. A splendid molecular machine. Annu. Rev. Biochem. **66**, 717–749
2 Dey, R. and Moraes, C. T. (2000) Lack of oxidative phosphorylation and low mitochondrial membrane potential decrease susceptibility to apoptosis and do not modulate the protective effect of Bcl-x(L) in osteosarcoma cells. J. Biol. Chem. **275**, 7087–7094
3 Harris, M. H., Vander Heiden, M. G., Kron, S. J. and Thompson, C. B. (2000) Role of oxidative phosphorylation in Bax toxicity. Mol. Cell Biol. **20**, 3590–3596
4 Matsuyama, S., Llopis, J., Deveraux, Q. L., Tsien, R. Y. and Reed, J. C. (2000) Changes in intramitochondrial and cytosolic pH: early events that modulate caspase activation during apoptosis. Nat. Cell. Biol. **2**, 318–325
5 Matsuyama, S., Xu, Q., Velours, J. and Reed, J. C. (1998) The mitochondrial F0F1-ATPase proton pump is required for function of the proapoptotic protein Bax in yeast and mammalian cells. Mol. Cell **1**, 327–336
6 Cuezva, J. M., Ostronoff, L. K., Ricart, J., López de Heredia, M., Di Liegro, C. M. and Izquierdo, J. M. (1997) Mitochondrial biogenesis in the liver during development and oncogenesis. J. Bioenerg. Biomembr. **29**, 365–377
7 Izquierdo, J. M. and Cuezva, J. M. (1997) Control of the translational efficiency of β-F1-ATPase mRNA depends on the regulation of a protein that binds the 3′-untranslated region of the mRNA. Mol. Cell Biol. **17**, 5255–5268
8 Izquierdo, J. M., Ricart, J., Ostronoff, L. K., Egea, G. and Cuezva, J. M. (1995) Changing patterns of transcriptional and post-transcriptional control of β-F1-ATPase gene expression during mitochondrial biogenesis in liver. J. Biol. Chem. **270**, 10342–10350
9 Luis, A. M., Izquierdo, J. M., Ostronoff, L. K., Salinas, M., Santarén, J. F. and Cuezva, J. M. (1993) Translational regulation of mitochondrial differentiation in neonatal rat liver. Specific increase in the translational efficiency of the nuclear-encoded mitochondrial β-F1-ATPase mRNA. J. Biol. Chem. **268**, 1868–1875
10 López de Heredia, M., Izquierdo, J. M. and Cuezva, J. M. (2000) A conserved mechanism for controlling the translation of β-F1-ATPase mRNA between the fetal liver and cancer cells. J. Biol. Chem. **275**, 7430–7437
11 Egea, G., Izquierdo, J. M., Ricart, J., San Martín, C. and Cuezva, J. M. (1997) mRNA encoding the β-subunit of the mitochondrial F1-ATPase complex is a localized mRNA in rat hepatocytes. Biochem. J. **322**, 557–565
12 Lithgow, T., Cuezva, J. M. and Silver, P. A. (1997) Highways for protein delivery to the mitochondria. Trends Biochem. Sci. **22**, 110–113
13 Ricart, J., Egea, G., Izquierdo, J. M., San Martín, C. and Cuezva, J. M. (1997) Subcellular structure containing mRNA for β-subunit of mitochondrial H^+-ATP synthase in rat hepatocytes is translationally active. Biochem. J. **324**, 635–643
14 Oleynikov, Y. and Singer, R. H. (1998) RNA localization: different zipcodes, same postman? Trends Cell. Biol. **8**, 381–383
15 Carson, J. H., Kwon, S. and Barbarese, E. (1998) RNA trafficking in myelinating cells. Curr. Opin. Neurobiol. **8**, 607–612
16 Kiebler, M. A. and DesGroseillers, L. (2000) Molecular insights into mRNA transport and local translation in the mammalian nervous system. Neuron **25**, 19–28
17 Bassell, G. J., Zhang, H., Byrd, A. L., Femino, A. M., Singer, R. H., Taneja, K. L., Lifshitz, L. M., Herman, I. M. and Kosik, K. S. (1998) Sorting of β-actin mRNA and protein to neurites and growth cones in culture. J. Neurosci. **18**, 251–265
18 Kohrmann, M., Luo, M., Kaether, C., DesGroseillers, L., Dotti, C. G. and Kiebler, M. A. (1999) Microtubule-dependent recruitment of Staufen-green fluorescent protein into large RNA-containing granules and subsequent dendritic transport in living hippocampal neurons. Mol. Biol. Cell **10**, 2945–2953
19 Marión, R. M., Fortes, P., Beloso, A., Dotti, C. and Ortin, J. (1999) A human sequence homologue of Staufen is an RNA-binding protein that is associated with polysomes and localizes to the rough endoplasmic reticulum. Mol. Cell Biol. **19**, 2212–2219
20 Wickham, L., Duchaine, T., Luo, M., Nabi, I. R. and DesGroseillers, L. (1999) Mammalian staufen is a double-stranded-RNA- and tubulin-binding protein which localizes to the rough endoplasmic reticulum. Mol. Cell Biol. **19**, 2220–2230
21 Di Liegro, C. M., Bellafiore, M., Izquierdo, J. M., Rantanen, A. and Cuezva, J. M. (2000) 3′-Untranslated regions of oxidative phosphorylation mRNAs function *in vivo* as enhancers of translation. Biochem. J. **352**, 109–115

22 Izquierdo, J. M. and Cuezva, J. M. (2000) Internal-ribosome-entry-site functional activity of the 3′-untranslated region of the mRNA for the β-subunit of mitochondrial H^+-ATP synthase. Biochem. J. **346**, 849–855

23 Danthinne, X., Seurinck, J., Meulewaeter, F., Van Montagu, M. and Cornelissen, M. (1993) The 3′-untranslated region of satellite tobacco necrosis virus RNA stimulates translation *in vitro*. Mol. Cell Biol. **13**, 3340–3349

24 Hann, L. E., Webb, A. C., Cai, J. M. and Gehrke, L. (1997) Identification of a competitive translation determinant in the 3′-untranslated region of alfalfa mosaic virus coat protein mRNA. Mol. Cell Biol. **17**, 2005–2013

25 Wang, S., Browning, K. S. and Miller, W. A. (1997) A viral sequence in the 3′-untranslated region mimics a 5′ cap in facilitating translation of uncapped mRNA. EMBO J. **16**, 4107–4116

26 Bashirullah, A., Cooperstock, R. L. and Lipshitz, H. D. (1998) RNA localization in development. Annu. Rev. Biochem. **67**, 335–394

27 Bassell, G. J., Oleynikov, Y. and Singer, R. H. (1999) The travels of mRNAs through all cells large and small. FASEB J. **13**, 447–454

28 Hazelrigg, T. (1998) The destinies and destinations of RNAs. Cell (Cambridge, Mass.) **95**, 451–460

29 Ades, I. Z. and Butow, R. A. (1980) The products of mitochondria-bound cytoplasmic polysomes in yeast. J. Biol. Chem. **255**, 9918–9924

30 Corral-Debrinski, M., Belgareh, N., Blugeon, C., Claros, M. G., Doye, V. and Jacq, C. (1999) Overexpression of yeast karyopherin Pse1p/Kap121p stimulates the mitochondrial import of hydrophobic proteins *in vivo*. Mol. Microbiol. **31**, 1499–1511

31 Corral-Debrinski, M., Blugeon, C. and Jacq, C. (2000) In yeast, the 3′-untranslated region or the presequence of ATM1 is required for the exclusive localization of its mRNA to the vicinity of mitochondria. Mol. Cell Biol. **20**, 7881–7892

32 Ellis, E. M. and Reid, G. A. (1993) The *Saccharomyces cerevisiae* MTS1 gene encodes a putative RNA-binding protein involved in mitochondrial protein targeting. Gene **132**, 175–183

33 Suissa, M. and Schatz, G. (1982) Import of proteins into mitochondria. Translatable mRNAs for imported mitochondrial proteins are present in free as well as mitochondria-bound cytoplasmic polysomes. J. Biol. Chem. **257**, 13048–13055

34 Zoladek, T., Vaduva, G., Hunter, L. A., Boguta, M., Go, B. D., Martin, N. C. and Hopper, A. K. (1995) Mutations altering the mitochondrial-cytoplasmic distribution of Mod5p implicate the actin cytoskeleton and mRNA 3′ ends and/or protein synthesis in mitochondrial delivery. Mol. Cell Biol. **15**, 6884–6894

35 Ni, L., Heard, T. S. and Weiner, H. (1999) *In vivo* mitochondrial import. A comparison of leader sequence charge and structural relationships with the *in vitro* model resulting in evidence for co-translational import. J. Biol. Chem. **274**, 12685–12691

36 Valcarce, C., Navarrete, R. M., Encabo, P., Loeches, E., Satrústegui, J. and Cuezva, J. M. (1988) Postnatal development of rat liver mitochondrial functions. The roles of protein synthesis and of adenine nucleotides. J. Biol. Chem. **263**, 7767–7775

37 Izquierdo, J. M. and Cuezva, J. M. (1993) Thyroid hormones promote transcriptional activation of the nuclear gene coding for mitochondrial β-F1-ATPase in rat liver. FEBS Lett. **323**, 109–112

38 Lee, J. H., Garboczi, D. N., Thomas, P. J. and Pedersen, P. L. (1990) Mitochondrial ATP synthase. cDNA cloning, amino acid sequence, overexpression, and properties of the rat liver α subunit. J. Biol. Chem. **265**, 4664–4669

39 Elkon, K. B., Parnassa, A. P. and Foster, C. L. (1985) Lupus autoantibodies target ribosomal P proteins. J. Exp. Med. **162**, 459–471

40 Marc, P., Margeot, A., Devaux, F., Blugeon, C., Corral-Debrinski, M. and Jacq, C. (2002) Genome-wide analysis of mRNAs targeted to yeast mitochondria. EMBO Rep. **3**, 159–164

41 Wachter, C., Schatz, G. and Glick, B. S. (1994) Protein import into mitochondria: the requirement for external ATP is precursor-specific whereas intramitochondrial ATP is universally needed for translocation into the matrix. Mol. Biol. Cell **5**, 465–474

42 Dibbens, J. A., Miller, D. L., Damert, A., Risau, W., Vadas, M. A. and Goodall, G. J. (1999) Hypoxic regulation of vascular endothelial growth factor mRNA stability requires the cooperation of multiple RNA elements. Mol. Biol. Cell **10**, 907–919

43 Grosset, C., Chen, C. Y., Xu, N., Sonenberg, N., Jacquemin-Sablon, H. and Shyu, A. B. (2000) A mechanism for translationally coupled mRNA turnover: interaction between the poly(A) tail and a c-*fos* RNA coding determinant via a protein complex. Cell (Cambridge, Mass.) **103**, 29–40

44 Gunkel, N., Yano, T., Markussen, F. H., Olsen, L. C. and Ephrussi, A. (1998) Localization-dependent translation requires a functional interaction between the 5′ and 3′ ends of oskar mRNA. Genes Dev. **12**, 1652–1664

45 Guo, L., Allen, E. M. and Miller, W. A. (2001) Base-pairing between untranslated regions facilitates translation of uncapped, nonpolyadenylated viral RNA. Mol. Cell **7**, 1103–1109

46 Thio, G. L., Ray, R. P., Barcelo, G. and Schupbach, T. (2000) Localization of gurken RNA in *Drosophila oogenesis* requires elements in the 5′ and 3′ regions of the transcript. Dev. Biol. **221**, 435–446

47 Johannes, G. and Sarnow, P. (1998) Cap-independent polysomal association of natural mRNAs encoding c-*myc*, BiP, and eIF4G conferred by internal ribosome entry sites. RNA **4**, 1500–1513

48 Hentze, M. W. (1997) eIF4G: a multipurpose ribosome adapter? Science **275**, 500–501

49 Preiss, T. and Hentze, M. W. (1999) From factors to mechanisms: translation and translational control in eukaryotes. Curr. Opin. Genet. Dev. **9**, 515–521

50 Tarun, Jr, S. Z. and Sachs, A. B. (1996) Association of the yeast poly(A) tail binding protein with translation initiation factor eIF-4G. EMBO J. **15**, 7168–7177

51 Ito, T., Tahara, S. M. and Lai, M. M. (1998) The 3′-untranslated region of hepatitis C virus RNA enhances translation from an internal ribosomal entry site. J. Virol. **72**, 8789–8796

52 Williamson, J. R. (2000) Induced fit in RNA–protein recognition. Nat. Struct. Biol. **7**, 834–837

53 Lipshitz, H. D. and Smibert, C. A. (2000) Mechanisms of RNA localization and translational regulation. Curr. Opin. Genet. Dev. **10**, 476–488

54 Fujiki, M. and Verner, K. (1991) Coupling of protein synthesis and mitochondrial import in a homologous yeast *in vitro* system. J. Biol. Chem. **266**, 6841–6847

55 Fujiki, M. and Verner, K. (1993) Coupling of cytosolic protein synthesis and mitochondrial protein import in yeast. Evidence for cotranslational import *in vivo*. J. Biol. Chem. **268**, 1914–1920

56 Funfschilling, U. and Rospert, S. (1999) Nascent polypeptide-associated complex stimulates protein import into yeast mitochondria. Mol. Biol. Cell **10**, 3289–3299

57 Ferro-Novick, S., Hansen, W., Schauer, I. and Schekman, R. (1984) Genes required for completion of import of proteins into the endoplasmic reticulum in yeast. J. Cell. Biol. **98**, 44–53

58 Schatz, G. and Dobberstein, B. (1996) Common principles of protein translocation across membranes. Science **271**, 1519–1526

Received 26 November 2001/20 March 2002; accepted 8 April 2002
Published as BJ Immediate Publication 8 April 2002, DOI 10.1042/BJ20011726